Supplementary Materials

Table S1. Chemical composition (Ni_2P content) of Ni_2P/P-GCN catalysts.

Sample	N (at. %)	Ni (at. %)	P (at. %)	Ni_2P content (wt.%)
5-Ni_2P/P-GCN	97.30	1.50	1.20	4.7
10-Ni_2P/P-GCN	95.18	3.34	1.48	10.2
15-Ni_2P/P-GCN	91.55	4.91	3.54	14.8
20-Ni_2P/P-GCN	90.19	6.79	3.02	19.5
15-Ni_2P/GCN_*b*	92.10	4.84	3.06	14.5
15-Ni_2P/P-GCN*	93.03	4.91	2.06	14.6

*Sample retrieved after catalytic recycle tests.

Table S2. Textural properties and energy band gap of GCN_*b*, GCN, P-GCN and Ni_2P/P-GCN materials.

Sample	BET surface area ($m^2\ g^{-1}$)	Pore volume ($cm^3\ g^{-1}$)	Pore size (nm)	Band gap (eV)
GCN_*b*	83	0.12	3.0	2.75
GCN nanosheets	113	0.18	3.4	2.81
P-GCN nanosheets	97	0.20	3.1	2.76
5-Ni_2P/P-GCN	92	0.15	3.2	2.74
10-Ni_2P/P-GCN	84	0.14	3.3	2.74
15-Ni_2P/P-GCN	75	0.12	3.3	2.73
20-Ni_2P/P-GCN	68	0.14	3.3	2.70

Table S3. Comparison of photocatalytic efficiency between 15-Ni_2P/P-GCN and other reported g-C_3N_4-based photocatalysts.

Photocatalyst	Reaction conditions	Photocatalytic degradation of Cr(VI)		Ref.
		C_t/C_0	Time (min)	
Biochar(40)/g-C_3N_4 NSs	**50 mg catalyst, 50 mL Cr(VI) solution (10 mg L^{-1}), 4-fluorophenol, 300 W Xe lamp (λ>420 nm), pH=2**	~70%	240	[59]
3.0 wt.% g-C_3N_4/MIL-53(Fe)	20 mg catalyst, 50 mL Cr(VI) solution (10 mg L^{-1}), 500 W Xe lamp, (420<λ<760 nm), pH=3	100%	180	[60]
Black P QDs/g-C_3N_4	50 mg catalyst, 50 mL $K_2Cr_2O_7$ solution (10 mg L^{-1}), 300 W Xe lamp, (λ>420 nm), pH=4.65	~95%	60	[61]
Porous (P, Mo)-doped/g-C_3N_x	0.05 g catalyst, 40 mL $K_2Cr_2O_7$ aqueous solution (100 mg/L), 0.03 g tartaric acid, 300 W xenon lamp equipped with a 420 nm cut-off filter	~95%	120	[62]
P-doped g-C_3N_4/SnS (30 wt.% SnS)	50 mg catalyst, 100 mL of $K_2Cr_2O_7$ (100 mg L^{-1}) solution, solar simulator with a low-pass cutoff filter (440 nm), pH=2	100%	60	[63]

HNO_3-treated g-C_3N_4	300 mg catalyst, 300 mL of 50 mg/L $K_2Cr_2O_7$ aqueous solution, 1 mL of 100 mg/mL citric acid aqueous solution, visible-light (λ>420 nm) irradiation, pH=3.2	100%	240	[64]
CoS_2/g-C_3N_4-rGO	10 mg catalyst, Cr(VI)-containing aqueous solution (20 mg/L, 20 mL) 350 W Xe lamp, pH=2	99.8%	120	[65]
Hydrothermal treated g-C_3N_4	300 mg catalyst, 300 mL of 50 mg/L $K_2Cr_2O_7$ aqueous solution, 1 mL of 100 mg/mL citric acid aqueous solution, visible-light (λ>420 nm) irradiation, pH=3.1	100%	150	[66]
Fe^0-doped g-C_3N_4/MoS_2	30 mg catalyst, 50 mL Cr(VI) solution (20 mg L^{-1}), RhB, 500 W Xe lamp (λ>420 nm)	91%	120	[67]
O and S co-dopped g-C_3N_4/Ni_2P	50 mg catalyst, 100 mL Cr(VI) (10 mg L-1), 50 mg citric acid, 300 W Xe lamp (λ>420 nm)	100 %	120	[68]
15-Ni_2P/P-GCN	**40 mg catalyst, 50 mL Cr(VI) solution (50 mg L^{-1}), 300 W Xe lamp, λ>360 nm, pH=2**	**>99%**	**80**	**In this work**

Table S4. PL lifetime biexponential decay model fitting parameters and calculated average carrier lifetimes for the GCN_*b*, GCN, P-GCN and Ni_2P-modified catalysts with 15 wt.% Ni_2P content.

Sample	τ_1 **(ns)**	τ_2 **(ns)**	α_1 **(%)**	α_2 **(%)**	τ_{av} **(ns)**
GCN_*b*	1.07	5.26	62.5	37.5	4.20
GCN	1.50	5.51	59.0	41.0	4.38
P-GCN	1.21	5.21	55.1	44.9	4.32
15-Ni_2P/P-GCN	2.03	6.58	60.8	39.2	5.11
15-Ni_2P/GCN_*b*	1.10	4.80	63.2	36.8	3.76

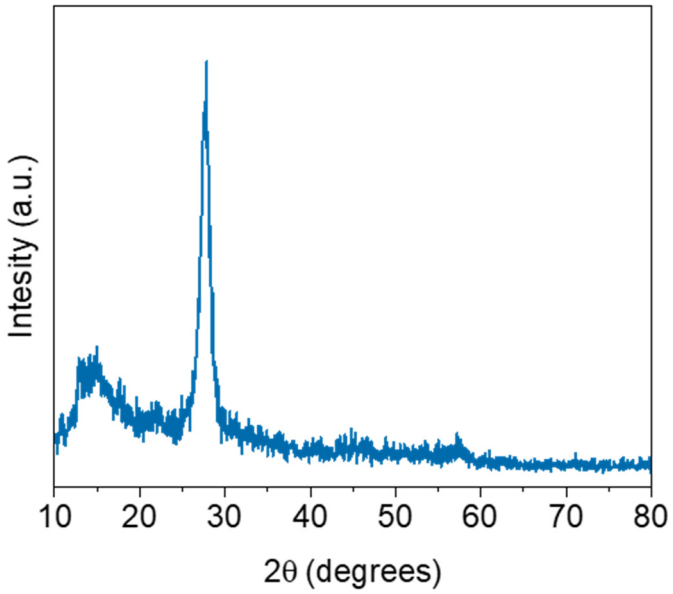

Figure S1. XRD pattern of P-dopped g-C_3N_4 (P-GCN). The broad feature at ~14.8° 2θ possibly comes from the unreacted phosphorus remained on the surface of g-C_3N_4.

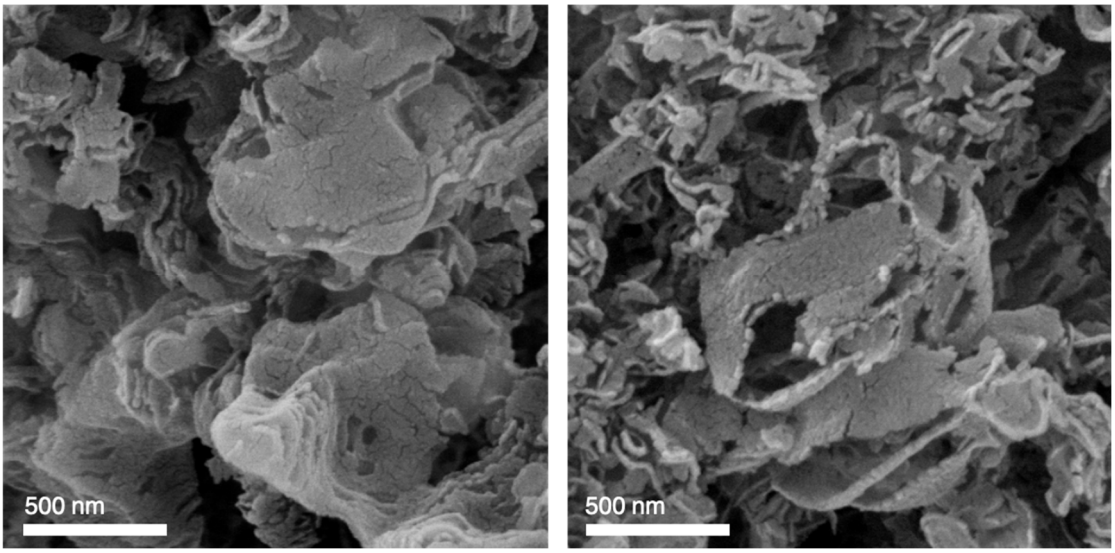

Figure S2. Typical FE-SEM images of as-made g-C_3N_4 (GCN_b).

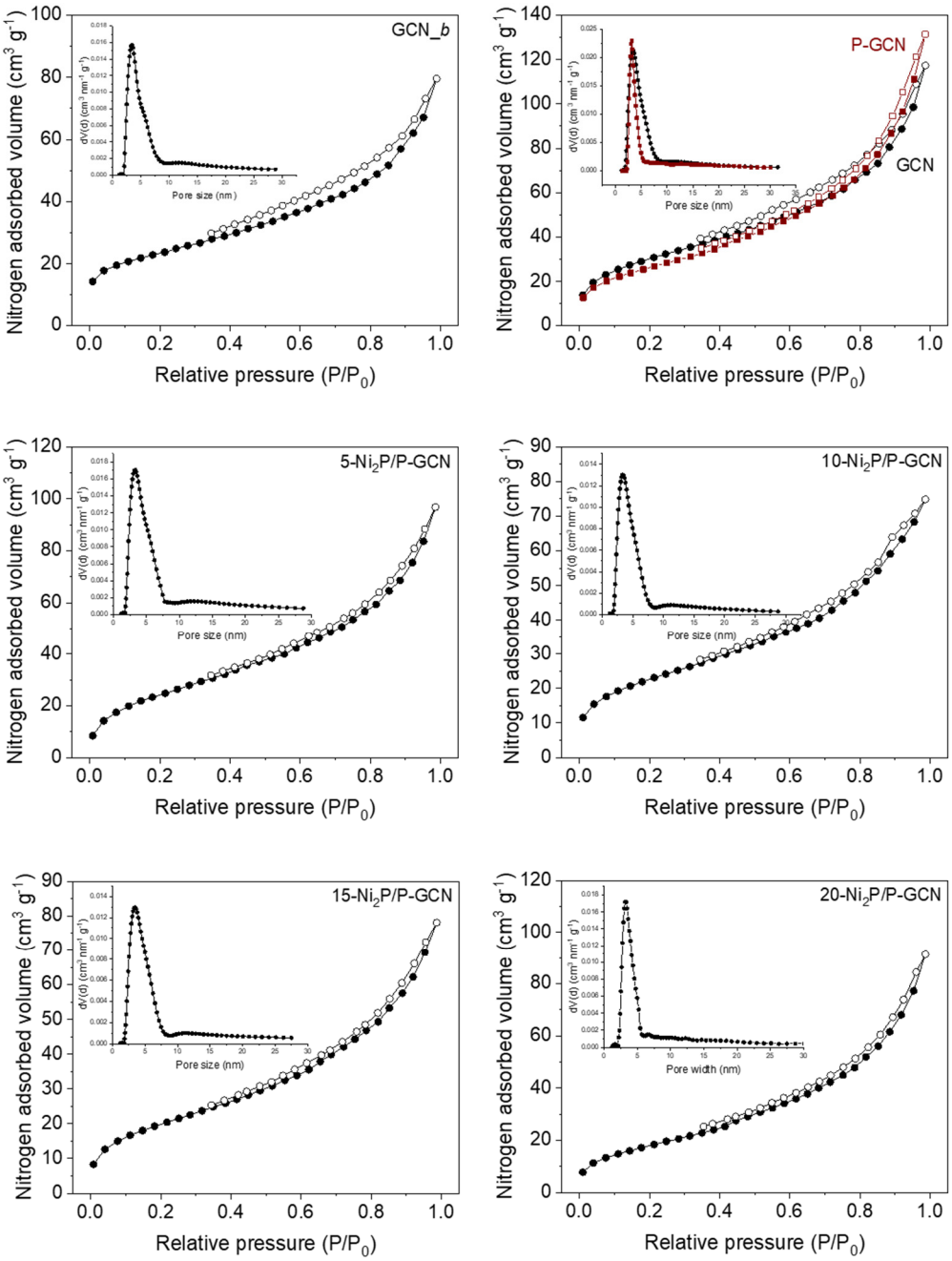

Figure S3. N_2 adsorption (filled cycles) and desorption (open cycles) isotherms at –196 °C and the corresponding NLDFT pore-size distribution plots (Insets) for the GCN_b, GCN, P-GCN and Ni_2P/P-GCN catalysts.

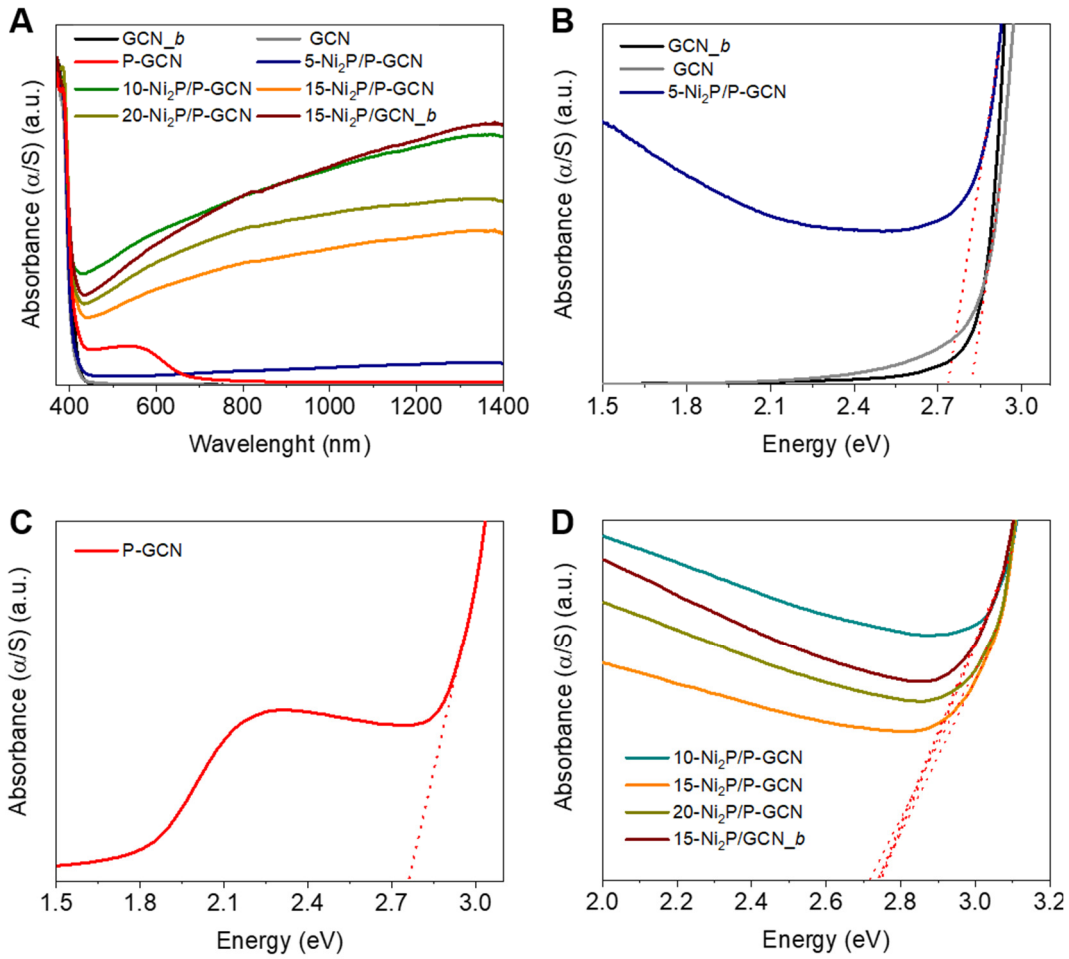

Figure S4. UV-vis/NIR absorption spectra versus wavelength (A) and photon energy (B-D) of the GCN_b, GCN and Ni2P/P-GCN and 15-Ni2P/GCN_b materials.

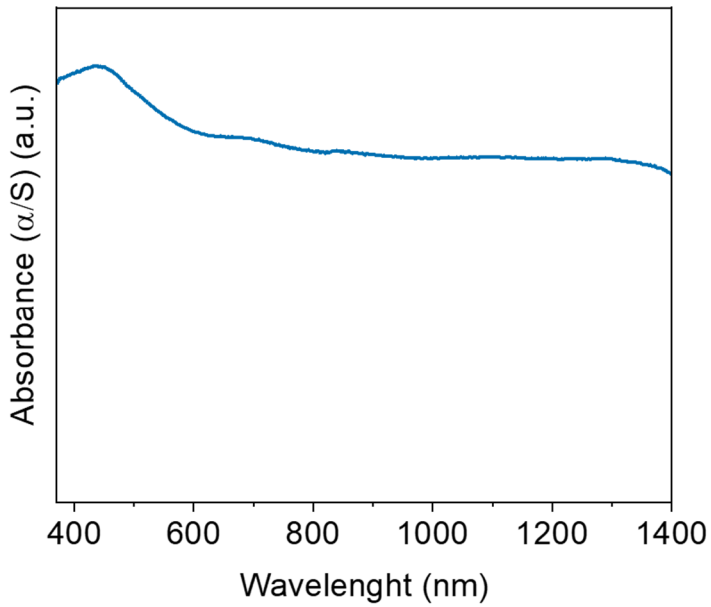

Figure S5. UV-vis/NIR absorption spectrum of the Ni2P particles.

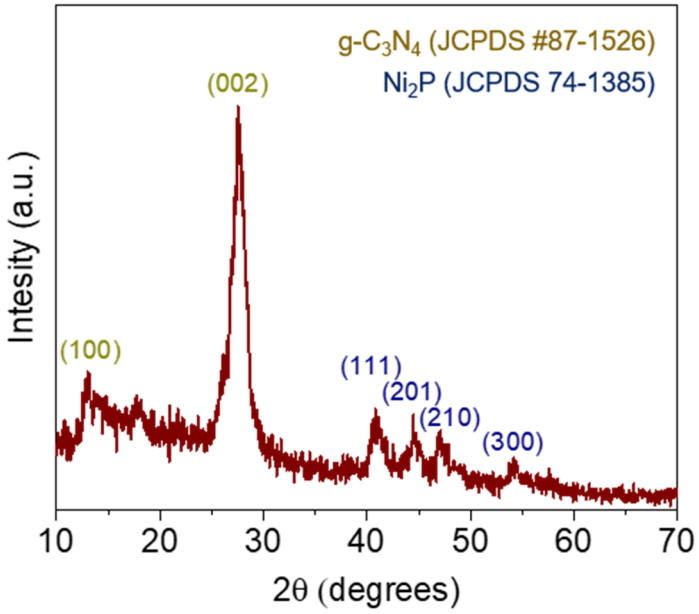

Figure S6. XRD pattern of the 15-Ni2P/GCN_*b* catalyst.

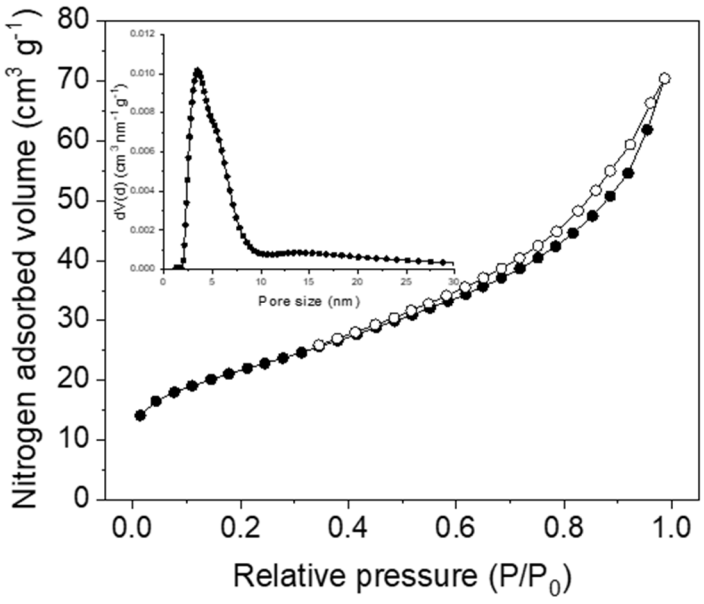

Figure S7. N_2 adsorption (filled cycles) and desorption (open cycles) isotherms –196 °C and the corresponding NLDFT pore-size distribution plot (Inset) for the 15-Ni2P/GCN_*b* catalyst. Analysis of the adsorption branch with the BET method gives surface area of 76 m^2g^{-1} and total pore volume of 0.11 cm^3g^{-1}. NLDFT pore size distribution calculated from the adsorption branch shows a maximum pore diameter of 3.5 nm.

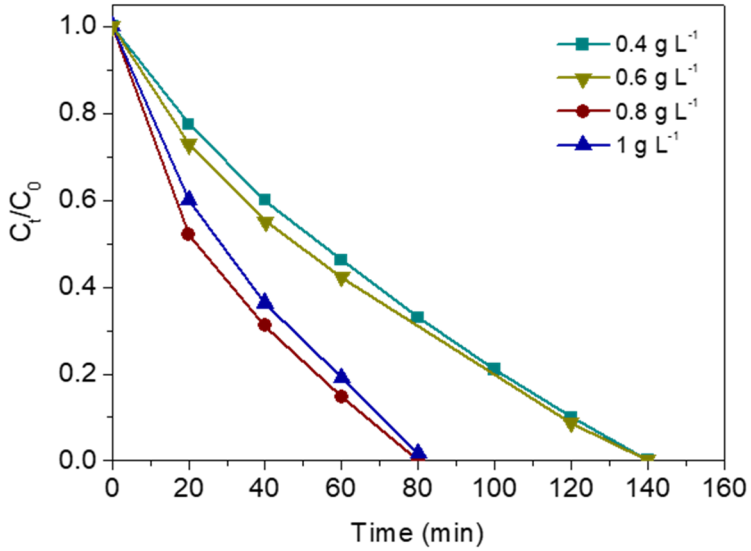

Figure S8. Concentration dependent photocatalytic Cr(VI) reduction activity of 15-Ni_2P/P-GCN catalyst. Reaction conditions: 0.4–1 g L^{-1} of catalyst, 50 mg L^{-1} Cr(VI) aqueous solution, pH = 2, UV-visible light (λ>360 nm) irradiation, 20 °C.

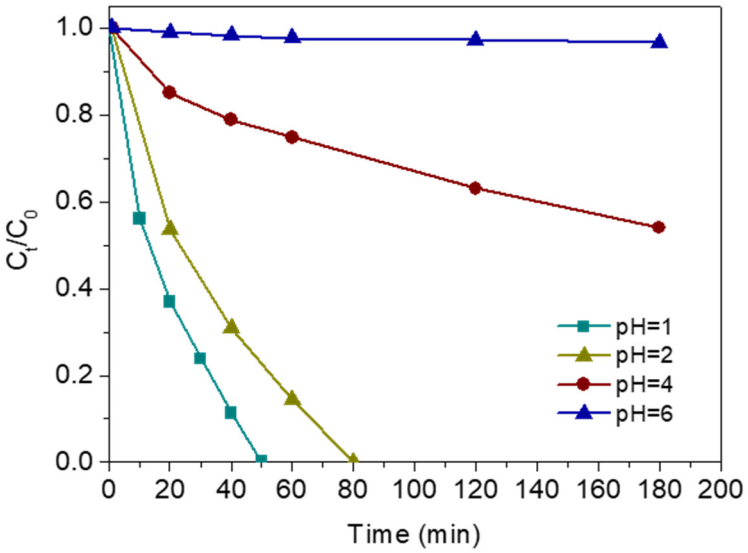

Figure S9. Effect of the solution pH on the photocatalytic Cr(VI) reduction performance. The photocatalytic reactions were performed as follows: 0.8 g L^{-1} catalyst, 50 mg L^{-1} Cr(VI) solution, pH = 2, λ > 360 nm light irradiation, 20 °C. The pH of the solution was adjusted with 2 M H_2SO_4 or 2 M NaOH.

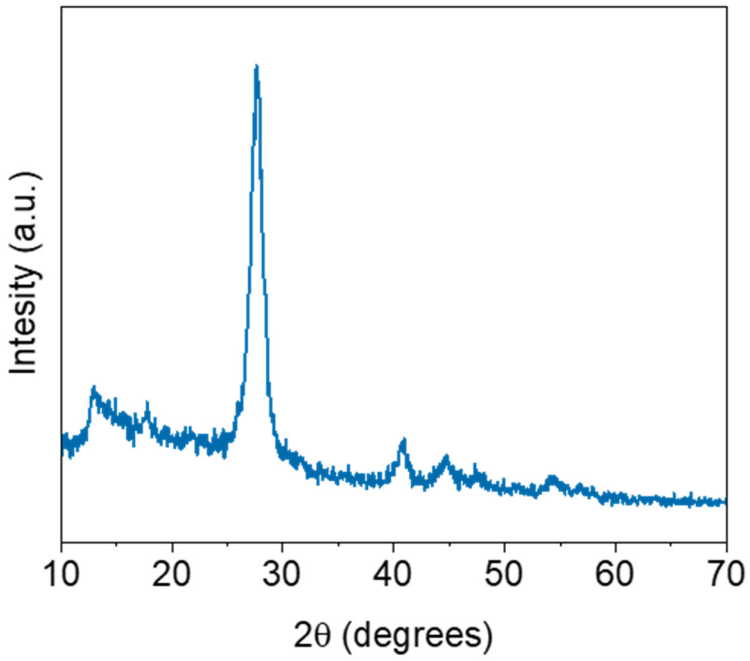

Figure S10. XRD pattern of the 15-Ni_2P/P-GCN catalyst after photocatalytic recycle tests.